Hindawi
Journal of Nanomaterials
Volume 2021, Article ID 6649200, 6 pages
https://doi.org/10.1155/2021/6649200

Research Article

Characteristics of Metal–Semiconductor–Metal Ultraviolet Photodetectors Based on Pure ZnO/Amorphous IGZO Thin-Film Structures

Kin-Tak Lam,[1] Sheng-Joue Young,[2] Yen-Lin Chu,[3] Chi-Nan Tsai,[3] Tung-Te Chu,[4] Ting-Sung Lu,[3] and Liang-Wen Ji[3]

[1]*Fujian University of Technology, Fuzhou, Fujian 350108, China*
[2]*Department of Electronic Engineering, National United University, Miaoli City 36063, Taiwan*
[3]*Department of Electro-Optical Engineering & Institute of Electro-Optical and Materials Science, National Formosa University, Yunlin 632, Taiwan*
[4]*Department of Mechanical Automation Engineering, Kao Yuan University, Kaohsiung 821, Taiwan*

Correspondence should be addressed to Sheng-Joue Young; youngsj@nuu.edu.tw, Yen-Lin Chu; 10576123@gm.nfu.edu.tw, and Liang-Wen Ji; lwji@nfu.edu.tw

Received 14 December 2020; Revised 15 January 2021; Accepted 31 March 2021; Published 12 April 2021

Academic Editor: Stefano Bellucci

In this study, metal–semiconductor–metal-structured ultraviolet (UV) photodetectors (PDs) based on pure zinc oxide (ZnO) and amorphous indium gallium zinc oxide (a-IGZO) thin films were fabricated and characterized. The ZnO seed layers were deposited on Corning glass substrates via a radio frequency (RF) magnetron sputtering technique. Results showed that under a 5 V applied bias; the dark currents of the pure ZnO and a-IGZO thin films were 0.112 pA and 2.85 nA, respectively. Meanwhile, the UV-to-visible rejection ratio of the pure ZnO and a-IGZO thin films were 14.33 and 256, respectively. Lastly, the PDs of thea-IGZO thin films had a lower leakage current and higher rejection ratio than that of the pure ZnO thin films from the UV to visible light region.

1. Introduction

In recent years, ultraviolet (UV) photodetectors (PDs) have played an important role in human health, ozone layer monitoring, and flame detection [1, 2]. Zinc oxide (ZnO) is a novel metal oxide semiconductor material that is used as an integral part of UV PDs [3, 4]. ZnO is an *n*-type and II-VI material; its bandgap is approximately 3.37 eV, and its excitation binding energy is 60 meV at room temperature [5, 6]. ZnO is a good crystallinity material. It has a hexagonal structure, and the lattice constants are $a = 3.24 - 3.26$ Å and $c = 5.13 - 5.43$ Å [7–9]. In addition, the lowest surface free energy of ZnO thin films lies on the (002) plane, and a good *c*-axis orientation can be obtained at a low temperature when ZnO thin films are grown. In addition to having good carrier mobility and photoelectric properties, crystalline metal oxide semiconductors are amorphous oxide semiconductor materials and thus have attracted considerable attention; moreover, the inclusion of ZnO compounds has led to extensive research. The type of material consists of various transition metals and oxygen atoms, such as zinc tin oxide (ZnSnO) [10], indium zinc oxide (InZnO) [11], and indium gallium zinc oxide (InGaZnO) [12], to enhance overall carrier mobility and photoelectric properties. Among them, the InGaZnO (IGZO) is a ternary oxide semiconductor. Its composition includes In_2O_3, Ga_2O_3, and ZnO. Amorphous IGZO oxide semiconductors have high carrier mobility, good uniformity, and wide energy bandgap, which offers good transparency in the visible spectrum; its peculiar chemical bonding instigates high field mobility and displays

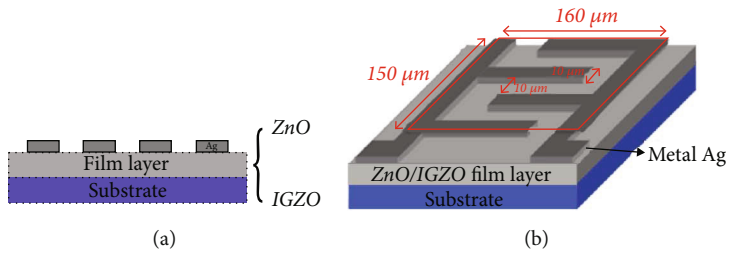

Figure 1: (Color online) (a) Side- and (b) top-view images of the IDT electrode.

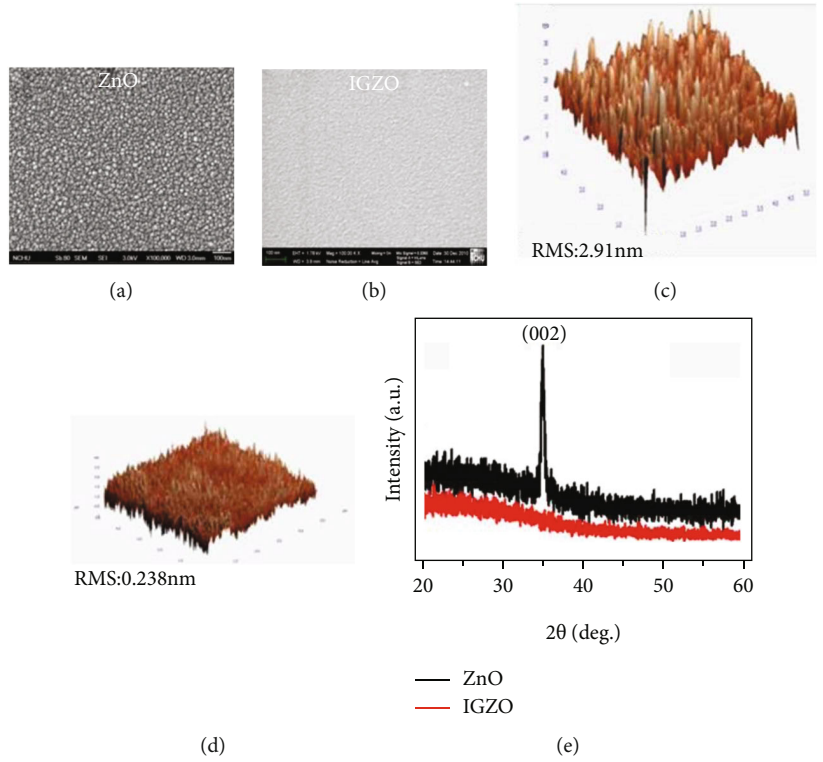

Figure 2: (a, b) SEM images of pure ZnO and a-IGZO thin films. (c, d) AFM images of 40 nm pure ZnO and 40 nm a-IGZO thin films. (e) XRD spectra of pure ZnO and a-IGZO thin films.

improved electrical characteristics, such as high I_{ON}/I_{OFF} ratio, enhanced lifetime, improved transmittance, and optimum large-area uniform integration [13–15]. The characteristics of transparency can be applied to the optical field.

In this study, the difference between crystalline ZnO thin-film PDs and amorphous IGZO thin-film PDs is discussed.

2. Experimental

Before UV PDs were manufactured, 1 cm × 1 cm Corning glass substrates were, respectively, cleaned for 10 min with acetone, isopropyl alcohol, and deionized water in an ultrasonic cleaner. Afterward, they were dried with flowing nitrogen and then placed in an oven for approximately 10 min at 45°C. Three-inch-diameter targets of pure ZnO and a-IGZO (atomic ratio In : Ga : Zn = 1 : 1 : 1) with a purity of 99.99% were used. The pure ZnO and a-IGZO thin films were grown using the radio frequency magnetron sputtering technique under a sputtering power of 100 W, a gas mixing ratio of Ar/O_2 (10/1), and a maintained chamber pressure at 5×10^{-2} Torr. The thickness was approximately 40 nm. Afterward, the film was annealed in a vacuum furnace at 450°C for 1 h to improve crystal quality. The resistivity of the pure ZnO thin films was ~10^{-5} (ohm-cm), and that of the a-IGZO thin films is approximately 1×10^{-3} (ohm-cm). The surface morphology, surface roughness, and crystallographic of the pure ZnO and a-IGZO thin films were characterized and explored by field-emission scanning electron microscopy (FE-SEM, JEOL JSM-6700F), atomic force microscopy (AFM, NT-MDT), and X-ray diffraction spectrum analysis with Cu Kα-1 radiation and $\lambda = 0.15405$ nm (XRD, MO3XHF22 MAC-Science), respectively. The optical characteristic was measured using a UV/visible spectrometer (UV-VIS, Hitachi U-2800).

In part of devices, the standard photolithography and lift-off were then performed to define the interdigitated (IDT)

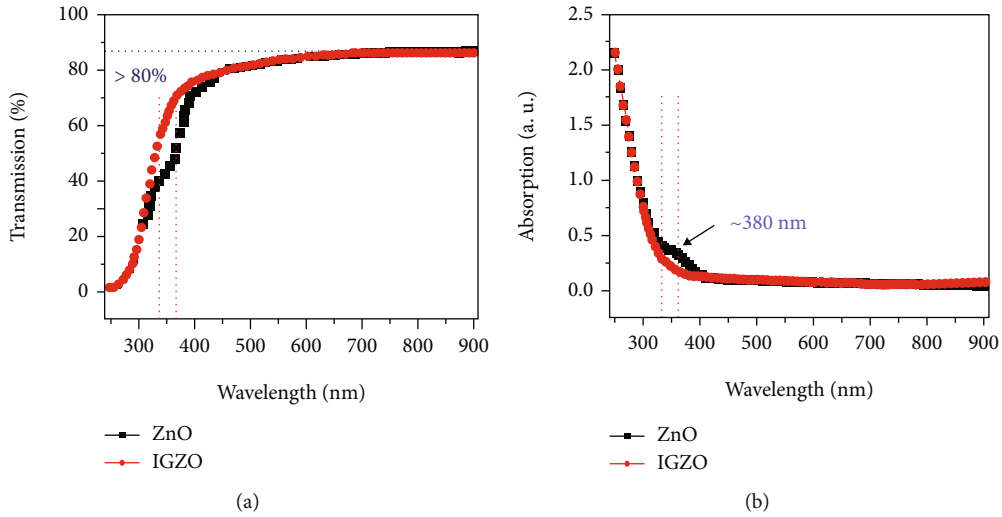

Figure 3: (a, b) Transmittance and UV-VIS spectra of pure ZnO and a-IGZO thin films.

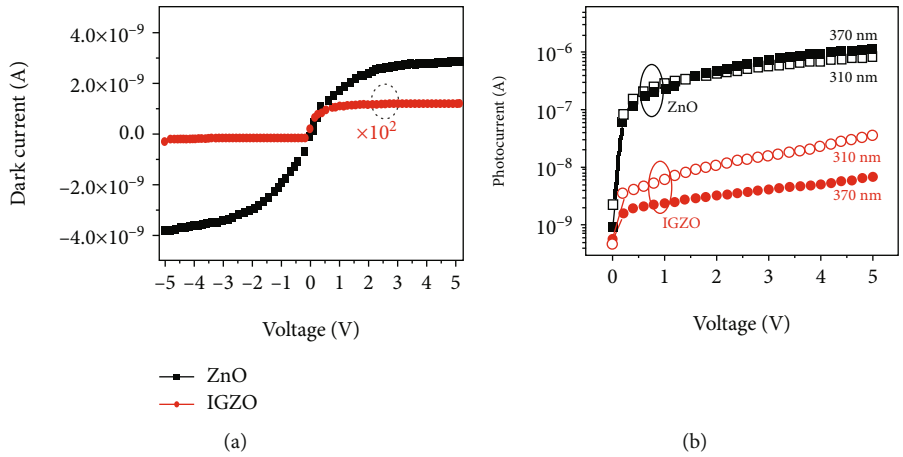

Figure 4: (a) Dark current–voltage (I–V) characteristics of the pure ZnO and a-IGZO thin films for UV PDs. (b) Photocurrent of pure ZnO and a-IGZO thin films at a wavelength 310 and 370 nm.

mask region. The IDT electrode measured 146, 10, and 10 μmin length, width, and space, respectively. The sensing active region was 150 μm × 160 μm. Subsequently, the silver (Ag) electrode was deposited by e-gun evaporation and used as contact electrode to form a metal–semiconductor–metal (MSM) structure, as shown in Figures 1(a) and 1(b). The light and dark currents of MSM UV PDs were measured by a semiconductor parameter analyzer (Agilent HP 4156C) system. The photoresponse was measured by a light source, i.e., a 300 W Xe lamp and a monochromator, from a 300–600 nm range. In this work, two MSM UV PD devices were fabricated to identify which is better.

Table 1: Dark current and photocurrent of the pure ZnO and a-IGZO thin films for UV PDs at 310 and 370 nm wavelengths.

Current (A)	Pure ZnO	a-IGZO
I_{dark}	2.85 nA	0.112 pA
$I_{ph(310\,nm)}$	0.82 μA	36.3 nA
$I_{ph(370\,nm)}$	1.1 μA	6.6 nA
$I_{ph(ZnO)}/I_{dark(ZnO)(370\,nm)}$	385.9	
$I_{ph(IGZO)}/I_{dark(IGZO)(370\,nm)}$	589.2	
$I_{ph(ZnO)}/I_{ph(IGZO)(310\,nm)}$	22.53	
$I_{ph(ZnO)}/I_{ph(IGZO)(370\,nm)}$	166.6	

3. Results and Discussion

Figures 2(a) and 2(b) show the surface morphology of pure ZnO and a-IGZO thin films by FE-SEM analysis and clearly indicate the difference between the surfaces of pure ZnO and a-IGZO. The pure ZnO film underwent grain formation, whereas the a-IGZO film did not. According to the AFM images shown in Figures 2(c) and 2(d), the surface roughness RMS value of the ZnO film was 2.91 nm, and that of the a-IGZO film was 0.238 nm, indicating that the overall surface of the pure ZnO film was rougher than the a-IGZO film because of grain formation. Figure 2(e) depicts the typical

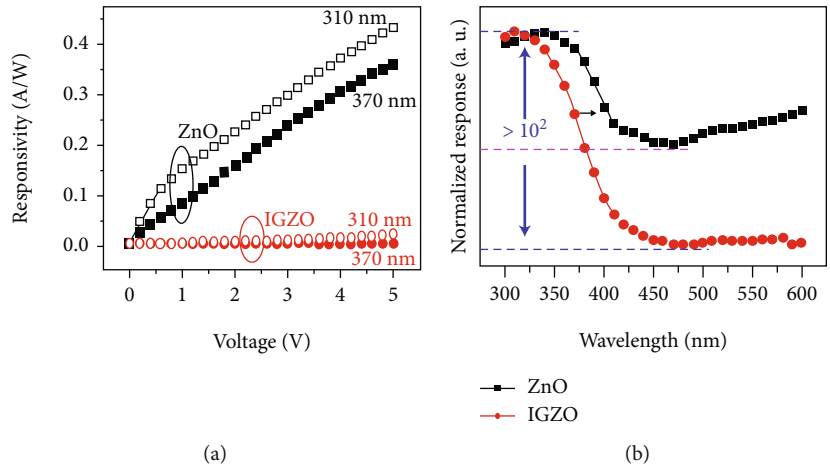

Figure 5: (a) Current responsivities of pure ZnO and a-IGZO thin films under different bias voltages. (b) Photoresponsivities of pure ZnO and a-IGZO thin films based on UV PDs at different wavelengths.

XRD results of the pure ZnO NRs and a-IGZO thin films that were prepared on the Corning glass substrate. The results indicated that the diffraction peak corresponded with the (002) planes. The peak revealed the hexagonal wurtzite structure of ZnO (JCPDS Card No. 36-1451) [16]. On the contrary, IGZO films showed amorphous phenomena [17].

Figures 3(a) and 3(b) show the spectrum of transmission and absorption of pure ZnO and a-IGZO thin films. Both had the same thickness of thin films, and the transmission could reach approximately 80% in the visible wavelength [18, 19]. However, the main difference was that the pure ZnO thin films slightly decayed in the 300–400 nm wavelengths. In the absorption spectrum, the absorption of the a-IGZO thin films was deeper than that of the pure ZnO thin films.

The measurements of the current–voltage (I–V) characteristics in pure ZnO and a-IGZO in the absence of light are shown in Figure 4(a). The dark current of the pure ZnO films was larger than that of the a-IGZO thin films because the a-IGZO thin films were amorphous. Therefore, in the a-IGZO thin films, the transmission path of relative current decreased, and the dark current would become relatively small under no effect by grain boundaries [20–22]. In the red parts of the figure, they are magnified to 10^2 times; the dark current was 0.112 pA under a 5 V applied bias. The black parts show the pure ZnO thin films; the dark current was 2.85 nA under a 5 V bias voltage. Similarly, the dark current of the former was larger than the latter by 256 times. Meanwhile, the pure ZnO thin films were in the (002) lattice direction. Therefore, the dark current would be evident under the transmission path of grain boundaries, indicating that the dark current would be restrained by an amorphous morphology. It was photocurrent in Figure 4(b). In the pure ZnO thin films, it was transferred in grain boundaries. Therefore, the dark current and the photocurrent became larger. As shown in Table 1, the semiconductor photocurrent I_{ph} is expressed as follows [23]:

$$I_{ph} = q\eta A\Phi_{ph}G \tag{1}$$

Table 2: Photoresponsivities of the pure ZnO and a-IGZO thin films for UV PDs.

Responsivity (R)	Pure ZnO/a-IGZO
$R_{310\,\mathrm{nm(ZnO)}}/R_{370\,\mathrm{nm(ZnO)}}$	1.22
$R_{310\,\mathrm{nm(IGZO)}}/R_{370\,\mathrm{nm(IGZO)}}$	10
$R_{310\,\mathrm{nm(ZnO)}}/R_{450\,\mathrm{nm(ZnO)}}$	14.33
$R_{310\,\mathrm{nm(IGZO)}}/R_{450\,\mathrm{nm(IGZO)}}$	256

where q is the electronic charge, η is the quantum efficiency, A is the active area, Φ_{ph} is the photon flux, and G is the photoconductive gain. The ratio of light current to dark current I_{ph}/I_{dark} was 589.2 in a-IGZO and 385.9 in pure ZnO; the former was larger than the latter. In addition, the photocurrent of the pure ZnO films was larger than the a-IGZO thin films, that is, approximately 166.6 times of $I_{ph(ZnO)}/I_{ph(IGZO)}$.

Figure 5(a) shows the current response value of pure ZnO and a-IGZO thin films at 310 and 370 nm wavelengths under a bias voltage of 0–5 V. Figure 5(b) shows the main photoresponsivity of parameter values in PDs. The UV-to-visible rejection ratio of a-IGZO PD was two orders more than that of pure ZnOPD from UV light to visible light, because the a-IGZO thin films were amorphous. This result indicates that the dark current and photocurrent would be restrained by an amorphous morphology, thus affecting the entire response. As shown in Table 2, the responsivity (R) of a PD is defined as follows [24, 25]:

$$R = \left(I_{light} - I_{dark}\right)/P_{opt} = I_{ph}/P_{opt}, \tag{2}$$

where I_{dark} is the dark current, I_{light} is the photocurrent, and P_{opt} is the incident optical power. The UV-to-visible rejection ratio of a-IGZO PD ($[R_{310\mathrm{nm\,(IGZO)}}/R_{450\mathrm{nm\,(IGZO)}}] = 256$)

was larger than that of pure ZnOPD ($[R_{310\text{nm(ZnO)}}/R_{450\text{nm(ZnO)}}] = 14.33$); in addition, the absorbance of UV light in the a-IGZO was deeper at a 310 nm wavelength.

4. Conclusion

The MSM structure of UVPDs based on pure ZnO and a-IGZO thin films was fabricated and characterized. Results showed that the dark currents of the pure ZnO and a-IGZO thin films were 0.112 pA and 2.85 nA, respectively, under a 5 V applied bias. Meanwhile, the UV-to-visible rejection ratios of the pure ZnO and a-IGZO thin film were 14.33 and 256, respectively. In the pure ZnO thin films, the dark current was evident under the transmission path of grain boundaries. Therefore, the dark current and photocurrent became larger. This result indicated that the dark current could be restrained by an amorphous morphology. Lastly, the PDs of the a-IGZO thin films had a lower leakage current and higher rejection ratio than that of the pure ZnO thin films from the UV to visible light region. In the future technology, the UV PDs can be combined with the Internet of Things and applied it to human skin to avoid skin aging and skin cancer.

Data Availability

All the data results in our article, we can provide them if requested.

Conflicts of Interest

The authors declare there are no competing interests.

Authors' Contributions

Yen-Lin Chu and Chi-Nan Tsai performed the experiments; Kin-Tak Lam, Sheng-Joue Young, and Liang-Wen Ji conceived the experiments; Tung-Te Chu and Ting-SungLu participated in data analysis.

Acknowledgments

This work was financially supported by the Ministry of Science and Technology of Taiwan (Project numbers MOST 107-2221-E-150-032, MOST 108-2221-E-024-006, MOST 108-2221-E-150-013-MY2, MOST109-2221-E-239-031-MY2, and MOST 106-2221-E-239-037-MY3). The authors would like to thank the Common Laboratory for Micro/Nano Science and Technology of the National Formosa University for the use of their measurement equipment and their assistance in this work; the Center for Micro/NanoScience and Technology, National Cheng Kung University, for device characterization; and C. N. Tsai for device fabrication and equipment support.

References

[1] M. Liao and Y. Koide, "High-performance metal-semiconductor-metal deep-ultraviolet photodetectors based on homoepitaxial diamond thin film," *Applied Physics Letters*, vol. 89, no. 11, article 113509, 2006.

[2] M. Razeghi and A. Rogalski, "Semiconductor ultraviolet detectors," *Journal of Applied Physics*, vol. 79, no. 10, pp. 7433–7473, 1996.

[3] Y.-L. Chu, S.-J. Young, R.-J. Ding, T.-T. Chu, T.-S. Lu, and L.-W. Ji, "Improving ZnO nanorod humidity sensors with Pt nanoparticle adsorption," *ECS Journal of Solid State Science and Technology*, vol. 10, no. 3, article 037003, 2021.

[4] Y. L. Chu, L. W. Ji, H. Y. Lu et al., "Fabrication and characterization of UV photodetectors with Cu-doped ZnO nanorod arrays," *Journal of The Electrochemical Society*, vol. 167, no. 2, article 027522, 2020.

[5] Y. L. Chu, S. J. Young, L. W. Ji, T. T. Chu, and C. H. Wu, "UV-enhanced field-emission performances of Pd-adsorbed ZnO nanorods through photochemical synthesis," *ECS Journal of Solid State Science and Technology*, vol. 10, no. 1, article 017001, 2021.

[6] Y.-L. Chu, S.-J. Young, L.-W. Ji et al., "Characteristics of gas sensors based on co-doped ZnO nanorod arrays," *Journal of The Electrochemical Society*, vol. 167, no. 11, article 117503, 2020.

[7] Y. L. Chu, S. J. Young, L. W. Ji, I. T. Tang, and T. T. Chu, "Fabrication of ultraviolet photodetectors based on Fe-doped ZnO nanorod structures," *Sensors*, vol. 20, no. 14, p. 3861, 2020.

[8] Y. L. Chu, S. J. Young, L. W. Ji, T. T. Chu, and P. H. Chen, "Synthesis of Ni-doped ZnO nanorod arrays by chemical bath deposition and their application to nanogenerators," *Energies*, vol. 13, no. 11, p. 2731, 2020.

[9] Y. L. Chu, L. W. Ji, Y. J. Hsiao et al., "Fabrication and characterization of Ni-doped ZnO nanorod arrays for UV photodetector application," *Journal of The Electrochemical Society*, vol. 167, no. 6, article 067506, 2020.

[10] L. Feng, G. Yu, X. Li, J. Zhang, Z. Ye, and J. Lu, "Solution processed amorphous ZnSnO thin-film phototransistors," *IEEE Transactions on Electron Devices*, vol. 64, no. 1, pp. 206–210, 2017.

[11] S. Sugumaran, M. N. B. Ahmad, M. F. Jamlos et al., "Transparent with wide band gap InZnO nano thin film: preparation and characterizations," *Optical Materials*, vol. 49, pp. 348–356, 2015.

[12] H. C. Wu and C. H. Chien, "Highly Transparent, high-performance IGZO-TFTs using the selective formation of IGZO source and drain electrodes," *IEEE Electron Device Letters*, vol. 35, no. 6, pp. 645–647, 2014.

[13] K. Nomura, H. Ohta, A. Takagi, T. Kamiya, M. Hirano, and H. Hosono, "Room-temperature fabrication of transparent flexible thin-film transistors using amorphous oxide semiconductors," *Nature*, vol. 432, no. 7016, pp. 488–492, 2004.

[14] J. Jeong, G. J. Lee, J. Kim, and B. Choi, "Electrical characterization of a-InGaZnO thin-film transistors with Cu source/drain electrodes," *Applied Physics Letters*, vol. 100, no. 11, article 112109, 2012.

[15] E. Fortunato, P. Barquinha, and R. Martins, "Oxide semiconductor thin-film transistors: a review of recent advances," *Advanced Materials*, vol. 24, no. 22, pp. 2945–2986, 2012.

[16] M. Suchea, S. Christoulakis, M. Katharakis, N. Katsarakis, and G. Kiriakidis, "Surface characterization of ZnO transparent thin films," *Journal of Physics: Conference Series*, vol. 10, pp. 147–150, 2005.

[17] C. M. Hsu, W. C. Tzou, C. F. Yang, and Y. J. Liou, "Investigation of the high mobility IGZO thin films by using co-sputtering method," *Materials*, vol. 8, no. 5, pp. 2769–2781, 2015.

[18] Y. Zhang, L.-X. Qian, Z. Wu, and X. Liu, "Amorphous InGaMgO ultraviolet photo-TFT with ultrahigh photosensitivity and extremely large responsivity," *Materials*, vol. 10, no. 2, p. 168, 2017.

[19] A. F. A. Razak, S. Devadason, C. Sanjeeviraja, and V. Swaminathan, "Effect of annealing on structural and optical properties of ZnO thin films by sol gel technique," *Chalcogenide Letters*, vol. 8, pp. 511–519, 2011.

[20] K. Nomura, A. Takagi, T. Kamiya, H. Ohta, M. Hirano, and H. Hosono, "Amorphous oxide semiconductors for high-performance flexible thin-film transistors," *Japanese Journal of Applied Physics*, vol. 45, no. 5B, pp. 4303–4308, 2006.

[21] H. Arora, P. E. Malinowski, A. Chasin et al., "Amorphous indium-gallium-zinc-oxide as electron transport layer in organic photodetectors," *Applied Physics Letters*, vol. 106, no. 14, article 143301, 2015.

[22] G. Wakimura, Y. Yamauchi, and Y. Kamakura, "Simulation and modeling of off-leakage current in InGaZnO thin-film transistors," *Journal of Advanced Simulation in Science and Engineering*, vol. 2, no. 1, pp. 201–210, 2015.

[23] S.-M. Peng, Y.-K. Su, L.-W. Ji et al., "Transparent ZnO nanowire-network ultraviolet photosensor," *IEEE Transactions on Electron Devices*, vol. 58, no. 7, pp. 2036–2040, 2011.

[24] Z.-H. Wang, H.-C. Yu, C.-C. Yang, H.-T. Yeh, and Y.-K. Su, "Low-frequency noise performance of Al-doped ZnO nanorod photosensors by a low-temperature hydrothermal method," *IEEE Transactions on Electron Devices*, vol. 64, no. 8, pp. 3206–3212, 2017.

[25] W. S. Shih, S. J. Young, L. W. Ji, W. Water, T. H. Meen, and H. W. Shiu, "Effect of oxygen plasma treatment on characteristics of $_{TiO$_{2}$}$ photodetectors," *IEEE Sensors Journal*, vol. 11, no. 11, pp. 3031–3035, 2011.